Evidence for Strong but Dynamic Iron−Humic Colloidal Associations in Humic-Rich Coastal Waters

ARTICLE *in* ENVIRONMENTAL SCIENCE & TECHNOLOGY · OCTOBER 2010

Impact Factor: 5.33 · DOI: 10.1021/es101081c · Source: PubMed

4 AUTHORS, INCLUDING:

François L L Muller
Qatar University
31 PUBLICATIONS **545** CITATIONS
SEE PROFILE

Chon-Lin Lee
National Sun Yat-sen University
59 PUBLICATIONS **830** CITATIONS
SEE PROFILE

Evidence for Strong but Dynamic Iron−Humic Colloidal Associations in Humic-Rich Coastal Waters

SILVIA BATCHELLI,[†] FRANÇOIS L. L. MULLER,*[,†] KUEI-CHEN CHANG,[‡] AND CHON-LIN LEE[‡]

Environmental Research Institute, Castle Street, Thurso, Caithness KW14 7JD, U.K., and Department of Marine Environment and Engineering, National Sun Yat-sen University, Kaohsiung 80424, Taiwan

Received April 6, 2010. Revised manuscript received June 29, 2010. Accepted October 4, 2010.

This study investigated the physicochemical forms of dissolved iron in the coastal plume (salinity = 28−35) of a small river draining a peat-rich catchment. Speciation information was obtained through a combination of fractionation by crossflow filtration (CFF) along with voltammetric detection of either naturally occurring iron−humic complexes (July survey) or known, synthetic complexes (September survey) formed by titrating the samples with the competing ligand 2-(2-thiazolylazo)-*p*-cresol (TAC). The majority of colloidal iron (>5000 Da) was present as iron−humic complexes supplied by the river and showing uniform conditional stability constants throughout the plume (log $K'_{Fe'HS}$ = 11.3 ± 0.1, i.e. log K_{Fe3+HS} = 21.3 ± 0.1). Noncolloidal or soluble iron was strongly complexed to ligands of marine origin with log $K'_{Fe'HS}$ = 11.9 ± 0.1. Equilibrium of the total iron pool with the added TAC ligand was achieved in all but the highest salinity sample, albeit more slowly for colloidal than for soluble iron. In addition, measurements of humiclike fluorescence suggested that the conformation of colloids could change over time as a result of dissociation of the iron−humic associations. These results are consistent with the concept that iron in coastal waters is strongly but reversibly bound to humic substances and therefore may be available for complexation by siderophore-type ligands released by microorganisms.

Introduction

Iron speciation in natural waters is both complex and fascinating as this element's chemistry is dominated by extensive hydrolysis but also organic complexation and redox transformations. Since J. H. Martin's demonstration of a link between iron bioavailability and phytoplankton growth in certain regions of the oceans (*1*), there has been an accumulation of evidence to suggest that iron may exert a significant control on oceanic primary production and nitrogen fixation at a global scale. However, our knowledge of the linkages between the oceanic iron and carbon cycles is still weak (*2*). Work in the estuarine and coastal environment ((*3*) and refs within) has focused mostly on the reactivity (aggregation and photochemical reactions) of colloidal iron oxide phases. However, some recent studies (*4*−*6*) have also revealed the existence of biologically derived Fe(III)-binding ligands, which can be produced by most heterotrophic and phototrophic marine bacteria to facilitate the solubilization and uptake of iron. One indication of the complexity of iron chemistry in seawater is that an inert pool of iron appears to coexist with the labile pool − especially in the coastal environment. Where it is found, this inert pool does not participate in the reactions taking place after an addition of iron (*7*) or strong iron-binding ligand (*8*). Resolution of this issue is further complicated by a lack of knowledge of the physicochemical form of this iron pool, which is attributed to solid phase oxyhydroxides by some authors (*8*) but to strong organic complexation by others (*7*). Notwithstanding the uncertainty about complexation and oxidation state of this inert pool, there is growing evidence that iron−colloid associations must play a part in preventing or retarding exchange between the various iron pools (*8*, *9*).

Recently, Laglera et al. (2007) developed a method to directly measure the concentration of humic and fulvic substances in coastal waters based on the iron-binding properties of these substances which were denoted collectively "HS" (*10*). Application of this method to waters of the Irish Sea revealed that humic-type substances could account for the total iron-binding capacity of these waters (*11*).

The present study was conducted in a nearly pristine coastal system influenced by a black water river known to form humic-rich buoyant plumes (*12*). Two surveys were conducted in July and September 2008 under similar and steady conditions of river discharge (3.2−4.4 m^3 s^{-1}). The main aim was to establish the physicochemical forms of iron throughout the coastal mixing zone (28 < S < 35) based on size fractionation by crossflow filtration (CFF) and detection of kinetically labile iron by adsorptive cathodic stripping voltammetry (ACSV). Particular attention was given to the colloid-solution partitioning of iron, its binding strength with natural organic ligands and the extent to which iron might be in a state of dynamic exchange between the colloidal and solution phase. Colloids were immersed by continuous diafiltration into both ultrafiltered, metal cleaned natural seawater (<1 kDa, iron stripped) and low ionic strength synthetic medium (0.01 M NH_4Cl) in an attempt to induce conformational changes. Their response to medium exchange was examined by voltammetric and/or fluorescence techniques. The results strongly suggest that iron and HS form dynamic associations in the colloidal size range. This iron is strongly bound to − and stabilized by − the HS component during advection and mixing of the plume.

Experimental Section

Materials. All reagents used in this study were of the highest purity available and are specified as they appear in the text. All solutions were prepared in high-purity water (Arium 611UV, Sartorius). All plastic-ware (HDPE) and Teflon-ware (PTFE or FEP) followed a rigorous cleaning protocol involving two extended soaks in detergent (Decon 5%) and HNO_3 (4 M, Fluka) baths, respectively. They were subsequently rinsed with high-purity water and allowed to dry in a Class 100 laminar flow cabinet (Bassaire) before being double wrapped in detergent-cleaned zip-lock polyethylene bags for storage. Metal-free seawater was generated through ultrafiltration (1 kDa) of seawater (S = 35) followed by a metal stripping step using 10 g/L of preconditioned Chelex-100 resin (Bio-Rad) in a batch mode (*13*).

* Corresponding author phone: +44-1847-889585 (ERI Thurso); e-mail: francois.muller@thurso.uhi.ac.uk.
[†] ERI Thurso.
[‡] NSYSU Kaohsiung.

10.1021/es101081c
Published on Web 10/21/2010

Study Site, Sampling, and Handling Procedures. Coastal seawater samples were collected from Thurso Bay during two surveys, July and September 2008, when the river flow was relatively low and constant (5 ± 0.2 m^3 s^{-1}) over the time scale of mixing in Thurso Bay ($\sim$ 24 h). Under these conditions, River Thurso exhibits typical dissolved iron concentrations of 3000−5000 nM (0.2−0.3 mg L^{-1}) and dissolved inorganic and organic concentrations of 8 and 16 mg L^{-1}, respectively (*12*). Under the same conditions, pH values of river water near the tidal limit are 7.6−8.4 (*12*) and suspended particulate matter (SPM) values are 1−3 mg L^{-1} (Scottish Environmental Protection Agency). This composition may explain why the bulk of dissolved iron is not prone to flocculation in the estuarine mixing zone (salinity range 0−30) of River Thurso, contrary to other peat-influenced river waters where the typical [Fe_T]/[DOC] ratio or SPM level are higher. The September plume survey was based on four sites across Thurso Bay covering roughly the same salinity range ($29.4 < S < 34.9$) as the samples that were collected in July ($29.3 < S < 34.4$) from four shore sites (Figure S1). Once in the laboratory, the samples were filtered within 2 h sequentially through a 0.8 μm cellulose acetate filter and a 0.40 μm hydrophilic polyethersulfone membrane through gentle vacuum filtration. All samples were ultrafiltered (5 kDa) within 4 days of collection and stored in the dark at 4 °C until analysis (except for the fluorescence subsamples, which were frozen). Samples for subsequent analysis of total iron were acidified with concentrated HNO_3 (TraceSelectUltra, Fluka) to a pH of approximately 1.8. The following determinations were made on the July fractionated samples (bulk, permeate, and retentate): ancillary variables, total iron ([Fe_T]), FeTAC complexes formed after an equilibration time of 0 h ([$FeTAC_0$]) and 14 h ([$FeTAC_{14}$]), and iron−humic complexes ([Fe−HS]). Size fractionated September samples were analyzed for: ancillary variables (including a_{355}), total iron concentration, total Fe-binding ligand concentration ([L_T]), conditional stability constant of the complex expressed with respect to either labile iron ($K_{Fe'L'}$) or free iron ($K_{FeL'}$), fluorescence intensities (I_F) at Ex/Em 370/450 and 370/500 nm, whose ratio is referred to in the literature as the fluorescence index, and humic and fulvic fluorescence intensities ($I_{267/450}$ and $I_{370/450}$) monitored versus reaction time in Chelex-100 batch experiments. Details of the analytical methods are provided in the Supporting Information. Measured values of the ancillary variables are presented in Table S1 of the Supporting Information(July) and Table 1 (September).

Cross-Flow Filtration Procedures. Samples were fractionated using a Sartorius Slice 200 benchtop cross-flow ultrafiltration system equipped with a peristaltic pump, Teflon tubing, polysulfone feed reservoir (500 mL capacity) and a 5 kDa Hydrosart cartridge with 0.1 m^2 surface area. The colloidal fraction, defined here as the material that passed through the 0.45 μm filter but now flows parallel to the CFF membrane with a nominal molecular weight (NMW) of 5 kDa, is recycled back into the reservoir. The fraction drawn from the reservoir at the end of the CFF operation is referred to as retentate and denoted R. The soluble fraction comprising low molecular weight (LMW) substances passing through the CFF membrane is denoted P. Colloidal fractions were isolated by continuous diafiltration in two contrasting exchange media. The first was ultrafiltered (1 kDa), metal-stripped seawater ($I = 0.6$ M, pH = 8.2), hereafter named R1. The second was a trace metal clean, 0.01 M ammonium chloride buffer (pH = 8.4), hereafter named R2. Full details of these procedures are presented in the Supporting Information.

Total Iron Determinations. The analysis of total iron was carried out either by adsorptive cathodic stripping voltammetry (ACSV) or inductively coupled plasma optical emission spectrometry (ICP-OES), either way no initial concentration

TABLE 1. Ancillary Variables and Measured and Calculated Iron-Binding Parameters for the Bulk (B), Permeate (P), and Retentate (R1, R2) Fractions of Each of the Four Samples Collected in Thurso Bay in September

code	latitude N	longitude W	T °C	salinity	pH	alkalinity μeq L^{-1}	a_{355} m^{-1}	F_{450}/F_{500}	[Fe_T] nmol L^{-1}	[L_T] nmol L^{-1}	log K	[Fe'_{calcd}][b] nmol L^{-1}	[Fe'_{meas}] nmol L^{-1}	[Fe_{noneq}][c] nmol L^{-1}
L1-B	58°36.059	03°30.767	13.5	32.0	7.93	2200	5.76	1.47	409.2 ± 48.1	385.2	11.75 ± 0.23	n.a.	0.046 ± 0.009	n.a.
L1-P	58°36.059	03°30.767		32.0	7.93			1.61	27.1 ± 0.8	67.0	11.18 ± 0.36	0.005 ± 0.003	0.006 ± 0.001	0.0 ± 6.0
L1-R1	58°36.059	03°30.767		35.3	8.10			1.52	316.8 ± 15.5	316.7	11.40 ± 0.19	0.420 ± 0.375	0.041 ± 0.008	14.5 ± 6.2
L1-R2	58°36.059	03°30.767		0.01 M[e]	8.35			1.30	213 ± 133	222.6	11.29 ± 0.20	0.042 ± 0.016	0.028 ± 0.006	8.5 ± 4.3
L2-B	58°36.091	03°30.704	13.9	29.4	8.06	2037	11.2	1.47	573.2 ± 17.4	604.4	11.12 ± 0.20	0.142 ± 0.054	0.142 ± 0.028	0.0 ± 18.4
L2-P	58°36.091	03°30.704		29.4	8.06			1.56	23.1 ± 1.2	46.5	10.23 ± 0.32	0.058 ± 0.030	0.041 ± 0.008	3.6 ± 8.9
L2-R1	58°36.091	03°30.704		35.3	8.10			1.44	367.0 ± 18.8	370.3	11.97 ± 0.91	0.126 ± 0.106	0.310 ± 0.062	n.a.
L2-R2	58°36.091	03°30.704		0.01 M	8.35			1.32	369.1 ± 11.4	398.3	11.05 ± 0.24	0.113 ± 0.047	0.095 ± 0.019	4.2 ± 12.3
L3-B	58°36.274	03°30.885	13.6	33.7	8.06	2284	1.38	1.54	240.0 ± 30.6	266.0	11.49 ± 0.30	0.030 ± 0.015	0.017 ± 0.003	16.5 ± 17.6
L3-P	58°36.274	03°30.885		33.7	8.06			1.64	52.2 ± 5.2	94.7	11.09 ± 0.26	0.006 ± 0.003	0.004 ± 0.001	12.6 ± 7.9
L3-R1	58°36.274	03°30.885		35.3	8.10			1.77	133.0 ± 10.0	80.9	n.a.	n.a.	0.015 ± 0.003	n.a.
L3-R2	58°36.274	03°30.885		0.01 M	8.35			1.35	51.5 ± 4.1	68.5	11.20 ± 0.15	0.019 ± 0.006	0.011 ± 0.002	7.9 ± 7.6
L4-B	58°37.395	03°31.891	13.6	34.9	8.08	2339	0.23	1.71	86.2 ± 9.4	102.1	11.72 ± 0.27	0.009 ± 0.004	0.003 ± 0.001	23.8 ± 18.4
L4-P	58°37.395	03°31.891		34.9	8.08			1.66	43.9 ± 1.4	93.2	11.93 ± 0.10	0.001 ± 0.000	0.008 ± 0.002	n.a.
L4-R1	58°37.395	03°31.891		35.3	8.10			1.98	63.7 ± 5.0	84.2	11.18 ± 0.18	0.021 ± 0.007	0.006 ± 0.001	23.8 ± 8.1
L4-R2	58°37.395	03°31.891		0.01 M	8.35			1.38	24.2 ± 0.6	70.7	11.32 ± 0.22	0.003 ± 0.001	0.001 ± 0.000	11.7 ± 4.6

[a] n.a. = not available. [b] Calculated by MINEQ+ using [Fe_T], [L_T], and $K_{Fe'}$ as inputs. [c] Represents the concentration that must be subtracted from [Fe_T] in order that [Fe'_{calc}] = [Fe'_{meas}]. [d] Note ± denotes the 95% confidence limits. [e] Medium for R2 was 0.01 M NH_4Cl adjusted to pH 8.4 with excess NH_3.

step was necessary. Comparative measurements were made between these two techniques as well as two different pretreatments, that is acidification to pH ~1.8 followed by storage for at least one week versus acidification and a short microwave treatment (*14*), to ensure the accurate determination of [Fe_T] that is essential for a meaningful characterization of iron chemistry. Full details are provided in the Supporting Information.

Direct Determination of Iron-Humic Species. Voltammetric experiments were performed using a 757 VA Computrace PC controlled system (Metrohm) housed inside a Class 100 laminar flow cabinet and equipped with a multimode electrode that combined the dropping mercury electrode (DME) and the stationary hanging mercury drop electrode (HMDE) in a single construction. The reference and the auxiliary electrodes were a double-junction Ag/AgCl (3 M KCl) and a platinum wire, respectively. Iron-humic complexes were determined by ACSV-monitored iron titrations according to the method of Laglera et al. (*10*) modified to adapt it to the high iron concentrations found in Thurso Bay. Full details can be found in the Supporting Information. The peak height for Fe−HS was found to increase linearly with the addition of iron within the full experimental range (0−80 nM) and so results are expressed here in equivalent [Fe−HS].

Determination of Iron Speciation by CLE-ACSV. Electrochemically labile fractions of iron − as well as Fe-complexing ligand concentrations and respective iron complex conditional stability constants ($K_{FeL'}$) − were determined by the method of Croot and Johansson (*8*). Their so-called labile Fe, Fe_{labile}, is denoted here $FeTAC_0$ to distinguish it from $FeTAC_{14}$ (the concentration of iron that is electrochemically labile after an equilibration time of 14 h). Single point measurements of [$FeTAC_0$] and [$FeTAC_{14}$] were carried out in July, and titrations with Fe at a fixed TAC concentration in September. Titrations with Fe allowed determination of the total concentrations and conditional stability constants of humic Fe-binding ligands, from which the proportion of iron occurring as Fe−HS in the original sample could be calculated. The analytical procedures, data interpretation and speciation calculations are described in the Supporting Information.

Fluorescence Measurements. Fluorescence emission spectra of the September samples were recorded with a Hitachi F-4500 equipped with a thermostatted cell holder. Excitation and emission slit widths were set at 5 nm. Except for when emission intensities were collected, the solutions were protected from light by a shutter device. In a preliminary step, scans were recorded with an excitation range set from 200 to 400 nm and an emission range set from 350 to 500 nm in 1 nm increment, to determine the peak positions for the humic and fulvic components expected to occur in those samples (*12*). The highest intensity peak was that of the humic component which peaked at Ex/Em 260−269/442−451 nm in each fraction (bulk, permeate, and retentate) of all samples. It is also worth noting here that the intensity of this peak was unaffected by additions of 1−5 μM Fe after overnight equilibration. From this point onward, only discrete fluorescence intensities were recorded. The fluorescence index defined as FI = $I_{370/450}/I_{370/500}$ (*15*) was measured in each fraction of every sample. In addition, variations of humic and fulvic fluorescence intensities measured at 267/450 and 370/450 nm respectively were monitored for up to five days in all the fractions while they were continuously reacted with 1% w/w of Chelex-100 resin (100−200 mesh designation, Bio-Rad) in a batch reactor mode. Full details can be found in the Supporting Information.

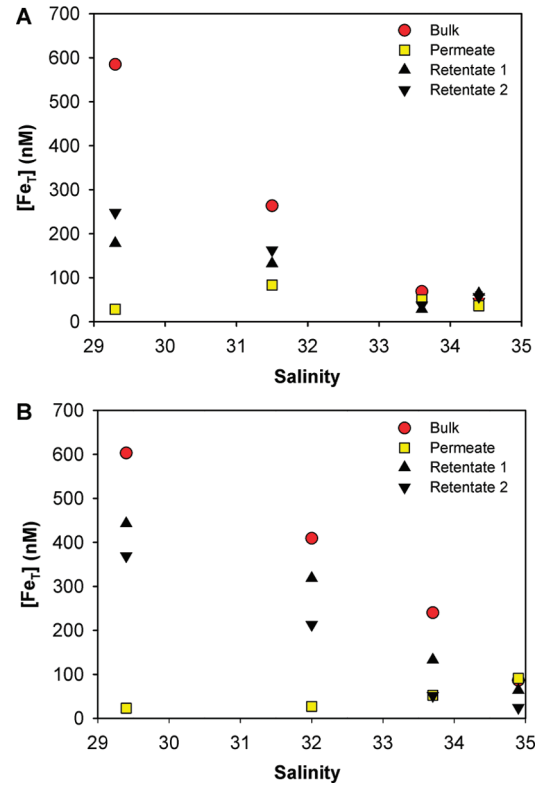

FIGURE 1. Total iron concentrations ([Fe_T]) across the salinity gradient encountered in Thurso Bay in July (A) and September (B).

Results and Discussion

Hydrographic and Water Quality Variables. Temperature, salinity and pH were measured in situ using a multiparameter environmental probe W23XD (Horiba Instruments). Salinities were chosen to cover the higher end of the mixing range (29 < S < 35), or far-field plume, where both colloidal and iron cycling processes are poorly understood. In both studies surface temperatures oscillated around 13.5 °C and pH varied between 7.9 and 8.4. Total alkalinity (TA) and absorption coefficient (a_{355}) were found to produce linear relationships with salinity in September (Figure S2 of the Supporting Information) − and probably also in July, given the similar river flow histories. This is indicative of conservative mixing of both inorganic and organic carbon between the riverine and marine end-members. These observations also imply that any chemical variable not producing a straight line when plotted against salinity must behave nonconservatively. Ancillary variables are listed in Table S1 of the Supporting Information (July) or Table 1 (September) along with the iron speciation data.

Distribution and Size Fractionation of Labile, Total and Humic-Bound Iron. Total (0.45 μm filtered, also denoted bulk) and colloidal (5 kDa − 0.45 μm, denoted retentate) iron concentrations measured by both ACSV and ICP-OES decreased approximately linearly with salinity (Figure 1) in July and September. A very slight curvature was observed in September (part B of Figure 1), perhaps indicating some small input of colloidal iron from the sediments at the end of the summer, that is after the main season of phytoplankton activity. In Liverpool Bay and the adjacent Irish Sea, a previous study (*11*) found evidence of removal of both Fe and HS in the salinity range 30.0 to 34.0. However, the distance of the mixing zone from the mouth of the Mersey estuary was 40 km while the offshore distance covered in our study was only 2 km. In Thurso Bay, total (bulk) and colloidal (retentate) iron concentrations covaried whereas soluble (permeate) iron levels were much smaller and uncorrelated.

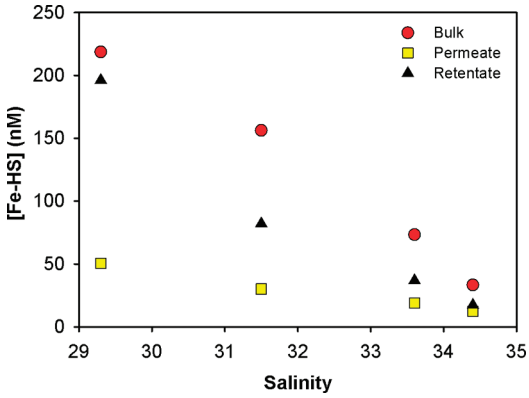

FIGURE 2. Humic-bound iron concentrations ([Fe−HS]) plotted as a function of salinity for each size fraction of the July samples.

It is clear from Figure 1 that the colloidal fraction contained a very significant portion of the total dissolved iron of these samples. Comparison with Figure 2 also suggests that the colloidal iron pool was mostly present as humic-bound iron. It was therefore not surprising to find that the colloidal phase also contained the majority of iron-binding ligands present in these samples (Table 1). Furthermore, the linear decrease of [Fe_T] and [Fe−HS] with salinity observed in the bulk and retentate fractions points clearly to a terrestrial origin for colloidal iron. These results are consistent with recent observations pointing to the importance of Fe−HS complexes in coastal waters (*10, 11*) as the most likely candidates to survive the precipitation reactions that tend to remove inorganic solid phases of iron from the water column (30).

A single source of soluble iron could not be established so unambiguously because variations observed along the salinity gradient in the permeate fraction were different in July and September. Both [Fe_T] (Figure 1) and [Fe−HS] (Figure 2) decreased linearly with salinity in the July permeate fractions whereas [Fe_T] increased with salinity in the September permeate fractions. This implies a terrestrial contribution to soluble iron in July and a marine contribution in September. Like colloidal iron, the land-derived soluble iron in July was bound to humic substances (Figure 2) which greatly enhanced the iron-carrying capacity of these waters. No direct determinations of Fe−HS species were made in September and so it is not possible to say whether the strong Fe-binding ligands measured in the September permeates (next section) were HS. Overall, the seasonal differences in the mixing behavior of soluble iron in this system could have been the result of seasonal fluctuations at the marine end-member or interchanges with the particulate or colloidal phase arising along the mixing gradient.

Source and Binding Strength of the Iron-Binding Ligands. Conditional stability constants for colloidal ligand complexation were essentially independent of salinity but constants for soluble ligand complexation showed an increasing trend toward higher salinities, from $\log K_{Fe'L'} = 10.23 \pm 0.32$ at $S = 29.4$ to $\log K_{Fe'L'} = 11.93 \pm 0.10$ at $S = 34.9$ (Table 1). This trend may indicate the presence of stronger ligands in the marine environment. Alternatively, it may have been due to the chemical heterogeneity of HS, that is the continuous distribution of functional groups of different binding strengths. According to this argument, however, an increase in $\log K_{Fe'L'}$ would have been brought about by a decrease in the fraction of occupied ligands, $[Fe_T]/[L_T]$: instead this ratio was remarkably uniform, with values of 0.50, 0.40, 0.55, and 0.47 respectively when progressing toward higher salinities. These soluble ligands were present in very small concentrations and so did not significantly influence the log $K_{Fe'L'}$ values measured in the filtered (bulk) samples (Table 1). Their high binding constants would tend to argue in favor of biological production (*4−6, 16*). For example, the release of siderophore with very high affinity for iron could enable marine bacteria to tap the relatively large iron store locked up in humic colloids. Such a release would likely be intermittent (to relieve iron stress) and highly localized (at hot spots at the colloid−water interface). It follows from this interpretation that there is not necessarily a contradiction between the detection of siderophores in Fe-stressed phytoplankton cultures (*5, 17*) or in open ocean waters (*6, 16*), and the contention by some authors that the bulk of the dissolved iron in seawater occurs as Fe−HS complexes (*11*). Given the relatively permeable structure of the humic-rich colloids (next section), siderophore production in the region of influence of River Thurso would be an efficient means to gain access to the main reservoir of iron (humic-rich colloids) in this environment.

As the proportion of seawater increases, DOM (bulk) becomes (a) less aromatic (as expected), (b) more fluorescent per mass of carbon (not shown) and (c) more iron-rich per mass of carbon or per unit absorbance (Table 1). The first observation is inferred from the increase in the fluorescence index, that is the ratio of the fluorescence emission intensity at a wavelength of 450 nm to that at 500 nm, obtained with an excitation of 370 nm (*14*); it indicates that the chemical nature of DOM changes from land-derived humic and fulvic material to compounds released in situ by biological production or decomposition processes. Observations (b) and (c) should be interpreted with caution. In particular, the use of fluorescence to distinguish the sources or chemical functionalities of DOM components can be complicated by aggregation and conformational changes in the colloidal fraction of the DOM (*12*), which here represents the dominant fraction.

Reversibility and Kinetics of Iron−Humic Complex (or Colloidal) Dissociation. It can be noted from the July study that the colloidal fraction contributed to the exchangeable (after 14 h equilibration) iron concentration [Fe_{TAC14}] to a greater extent than it did to the labile iron concentration [Fe_{TAC0}] (Figure S3 of the Supporting Information). This shows that the rate of dissociation of the iron−humic colloidal associations was delayed compared to soluble iron organic complexes, as would be anticipated if a portion of the iron was buried inside the colloidal matrix. Despite this kinetic limitation, it is worth reminding ourselves (September study) that the entire pool of colloidal iron could be successfully modeled as being at equilibrium with a single ligand type with the possible exception of the highest salinity sample. In that sample, a small but significant portion of colloidal iron was inert to ligand exchange (Table 1), as was recently reported in other studies (*7, 9*). In all but the highest salinity sample, however, dissociation from the humic colloids appeared to be entirely reversible. Additionally, it was found that [Fe′] had essentially the same value in the retentate (R1 or R2) harvested after diafiltration as in the bulk sample (Table 1), which again suggests some dynamic equilibrium between colloidal and soluble iron such that this equilibrium would appear to be re-established upon immersion of the colloids in a new, iron-stripped medium.

As noted above, the exception to this reversible behavior occurred in the highest salinity sample with the presence of an unreactive iron pool found principally in the colloidal phase. This unreactive pool must have been of marine origin as it represented 1% of the colloidal iron at $S = 29.4$, 4% at $S = 32.0$, 15% at $S = 33.7$ and 48% at $S = 34.9$ (Table 1, R2 values). It accounted for the increasing discrepancy between [Fe'_{meas}] and [Fe'_{calc}] in the bulk and retentate fractions toward increasing salinities, that is decreasing concentrations (Figure 3). The existence of this kinetically inert pool has implications for the accurate determination of iron speciation (*18*) because the latter is generally based on the assumption that the entire

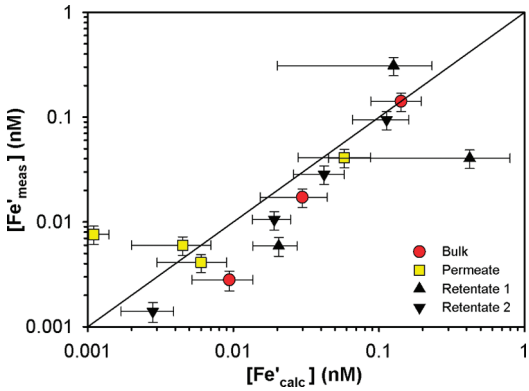

FIGURE 3. Relationship between measured and calculated labile iron concentrations in the bulk and size-fractionated samples collected in September. [Fe′$_{calc}$] was calculated by MINEQL+ using [Fe$_T$], [L_T], and $K_{Fe'}$ as inputs.

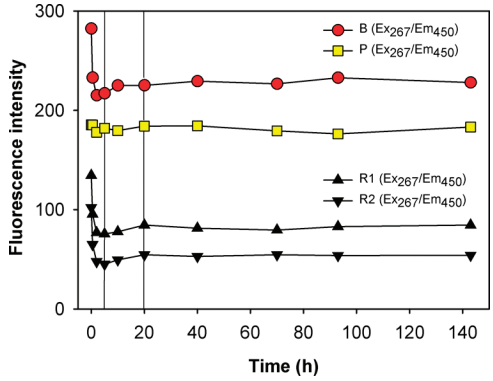

FIGURE 4. Representative plots of the changes in humic fluorescence intensity occurring during batch treatment with Chelex-100 resin, as illustrated here by Sample L1.

pool of iron is involved in ligand exchange reactions. If an inert pool of iron is present, equilibrium binding parameters calculated using total iron concentration may not be valid. Another consequence may be a reduction in biological uptake (*19, 20*) due to kinetic inertness.

Given that humic colloids in this coastal environment were found to carry relatively large concentrations of iron, it was deemed possible that iron could influence the conformation of humic molecules and perhaps their degree of aggregation. Therefore, a kinetic experiment was carried out in an effort to gain insight into the fate and transformation of the DOM matrix as iron was removed from it with a synthetic ligand. Experimental details and raw data from this uptake experiment are presented in Table S2 of the Supporting Information. In short, each fraction (B, P, R1, R2) of samples L1, L3 and L4 of the September survey were reacted with Chelex-100 resin for up to 140 h while the fluorescence intensities (I_F) at Ex/Em 267/450 and 370/450 nm were monitored over the course of the experiment. The most striking feature was that I_F remained constant throughout the 140 h period in the P fractions but showed an exponential initial decrease from 0−2 h followed by a slower increase toward a new equilibrium from 5−20 h in the B, R1, and R2 fractions. Results from sample L1 are shown as an example in Figure 4. The initial decrease, which was independent of excitation wavelength and was greatest in the R2 fractions, was likely an artifact caused by coagulation or adsorption of the larger colloids induced by the chelating resin beads. The subsequent increase in I_F was on the order of 2−8% at Ex/Em 267/450 (i.e., in the humic region), except in 3R2 and 1R2 where it was 16% and 19%, respectively. Two possible mechanisms for the increase in I_F can be envisaged: (a) an effect proportional to the removal of iron (*21*−*23*), for example the I_F enhancement of initially Fe-quenched components (if so, it should also have occurred in the soluble fraction), and (b) an indirect consequence of the removal of iron, perhaps a loosening or breakup of humic colloids leading to changes in the molecular environment of the fluorescent sites (*24*): according to this mechanism, exposure to the low ionic strength medium (R2) would have modified the 3D structure of the colloids, thus enhancing the fluorescence intensity of some fluorophores preferentially.

Analytical and Environmental Significance. There has been an increase in the popularity of fluorescence techniques in the aquatic sciences in the last 15 years. Some major applications have been in the characterization of DOM composition and source. In the last 10 years or so, the effect of metals on the natural fluorescence of DOM has been investigated in laboratory experiments (*22*−*24*). It should be emphasized, however, that the apparent covariation between dissolved iron concentration and humic-type fluorescence observed in Thurso Bay does not imply that iron-binding and fluorescent sites coincide, as recently noted by Laglera et al. (*10*) in their study of Liverpool Bay and the adjoining Irish Sea. Indeed, the most abundant iron-binding ligands in the humic-rich coastal waters examined here were found in the colloidal phase, whereas the most highly fluorescent fraction of DOM was actually the soluble phase. Nevertheless, an indirect link does seem to exist between the bulk fluorescence of DOM and the stabilization of colloids by iron, although evidence for this link is only revealed when iron levels are brought down to much lower values (i.e., after 5 h of reaction with Chelex-100 resin) or boosted to much higher levels (i.e., somewhere above 5 μM) than ambient. It follows that in this coastal system, and probably others, the fluorescence properties of HS are very unlikely to be altered by natural variations in total iron concentrations, which means that only the actual concentration of DOM contributes to the humic fluorescence signature. On the other hand, there is documented evidence that the molecular weight of naturally occurring colloids may affect the fluorescence spectrum of DOM in natural waters (*12, 25*). This is why the combination of CFF fractionation with voltammetric and fluorescence techniques offers the hope to better understand the role of iron in controlling colloidal DOM biogeochemical reactivity in coastal and nearshore waters.

Many higher latitude areas of Asia, Europe, and North America contain much larger humic-rich rivers than River Thurso which link vast peatland carbon stores to the marine environment, creating DOM-rich plumes at the freshwater−marine interface. Currently, we know little about the fate of riverine carbon and iron in the marine environment. We have known for some time, however, that iron occurs largely in colloidal forms and also that humic material, which degrades only slowly, can protect iron against coagulation by expanding the effective distance between approaching colloids as well as by altering their net surface electrostatic charge (*26, 27*). In the present study, we have shown that the portion of iron that has survived flocculation in the estuarine mixing zone − which is nearly 100% of the iron initially dissolved in River Thurso (unpublished results) but can be significantly less in other systems (*28, 29*) − is for the most part very strongly held in iron−humic colloidal associations which stay as dispersed colloids (i.e., as part of operationally dissolved Fe) under marine conditions. This lends support to recent suggestions that humic colloids may constitute an important carrier of dissolved iron to the continental shelf (*10, 29*) and perhaps to the open ocean (*11*). Furthermore, we have shown that these colloidal associations, which may (July survey) or may not (September survey) also contain oxide microparticles, can be broken up and the iron be slowly but quantitatively exchanged with the soluble phase upon addition of a high-affinity synthetic ligand. This suggests that

iron bound in these colloidal forms might be accessible to microorganisms relying on siderophore-based transport systems, for example many cyanobacteria (*16, 17*). Heterotrophic bacteria would perhaps also be able to exploit this source of iron if the colloids self-aggregated or became trapped within an organic meshwork, such as that produced by phytoplankton exudates.

Acknowledgments

This work was supported by the UHI Millennium Institute's ARC Program, a joint funding initiative sponsored by Highland and Islands Enterprise, the Scottish Funding Council, the European Regional Development Fund and the Natural Environment Research Council (NE/C510532/1). The fluorescence measurements were made possible thanks to an International Exchange Grant from the Royal Society of Edinburgh that covered the trip by F. L. L. Muller to the National Sun Yat-sen University, Taiwan. An earlier version of this article was vastly improved thanks to the comments made by three anonymous reviewers.

Supporting Information Available

Map of the sampling sites and a description of the sampling method, CFF operating parameters, analytical methods, and iron speciation calculations. This material is available free of charge via the Internet at http://pubs.acs.org.

Literature Cited

(1) Martin, J. H.; Fitzwater, S. E. Iron deficiency limits phytoplankton growth in the northeast Pacific Subarctic. *Nature* **1988**, *331*, 341–343.

(2) *The Biogeochemistry of Iron in Seawater*; Turner, D. R., Hunter, K. A., Eds.; IUPAC Series on Analytical and Physical Chemistry of Environmental Systems, Vol. 7; John Wiley & Sons: Chichester, 2001.

(3) Moffett, J. M. Transformations amongst different forms of iron in seawater. In *The Biogeochemistry of Iron in Seawater*; Hunter, K. A., Turner, D. R., Eds.; John Wiley & Sons: Chichester, 2001; pp 343−373.

(4) Barbeau, K.; Rue, E. L.; Bruland, K. W.; Butler, A. Photochemical cycling of iron in the surface ocean mediated by microbial iron(III)-binding ligands. *Nature* **2001**, *413*, 409–413.

(5) Barbeau, K.; Rue, E. L.; Trick, C. G.; Bruland, K. W.; Butler, A. Photochemical reactivity of siderophores produced by marine heterotrophic bacteria and cyanobacteria based on characteristic Fe(III) binding groups. *Limnol. Oceanogr.* **2003**, *48*, 1069–1078.

(6) Mawji, E.; Gledhill, M.; Milton, J. A.; Tarran, G. A.; Ussher, S.; Thompson, A.; Wolff, G. A.; Worsfold, P. J.; Achterberg, E. P. Hydroxamate siderophores: Occurrence and importance in the Atlantic Ocean. *Environ. Sci. Technol.* **2008**, *42*, 8675–8680.

(7) Gerringa, L. J. A.; Rijkenberg, M. J. A.; Wolterbeek, H. T.; Verburg, T. G.; Boye, M.; de Baar, H. J. W. Kinetic study reveals weak Fe-binding ligand, which affects the solubility of Fe in the Scheldt estuary. *Mar. Chem.* **2007**, *103*, 30–45.

(8) Croot, P. L.; Johansson, M. Determination of iron speciation by cathodic stripping voltammetry in seawater using the competing ligand 2-(2-thiazolylazo)-p-cresol (TAC). *Electroanalysis* **1999**, *12*, 565–576.

(9) Cullen, J. T.; Bergquist, B. A.; Moffett, J. W. Thermodynamic characterization of the partitioning of iron between soluble and colloidal species in the Atlantic Ocean. *Mar. Chem.* **2006**, *98*, 295–303.

(10) Laglera, L. M.; Battaglia, G.; van den Berg, C. M. G. Determination of humic substances in natural waters by cathodic stripping voltammetry of their complexes with iron. *Anal. Chim. Acta* **2007**, *599*, 58–66.

(11) Laglera, L. M.; van den Berg, C. M. G. Evidence for geochemical control of iron by humic substances in seawater. *Limnol. Oceanogr.* **2009**, *54*, 610–619.

(12) Batchelli, S.; Muller, F. L. L.; Baalousha, M.; Lead, J. R. Size fractionation and optical properties of colloids in an organic-rich estuary (Thurso, UK). *Mar. Chem.* **2009**, *113*, 227–237.

(13) Muller, F. L. L.; Kester, D. R. Measurement of the different forms of zinc in Narragansett Bay water based on the rate of uptake by a chelating resin. *Mar. Chem.* **1991**, *33*, 71–90.

(14) Bruland, K. W.; Rue, E. L. Analytical methods for the determination of concentrations and speciation of iron. In *The Biogeochemistry of Iron in Seawater*; Turner, D. R., Hunter, K. A., Eds.; John Wiley & Sons: Chichester, 2001; pp 255−289.

(15) McKnight, D. M.; Boyer, E., W.; Westerhoff, P. K.; Doran, P. T.; Kulbe, T.; Andersen, D. T. Spectrofluorometric characterization of dissolved organic matter for indication of precursor organic material and aromaticity. *Limnol. Oceanogr.* **2001**, *46*, 38–48.

(16) Martinez, J. S.; Zhang, G. P.; Holt, P. D.; Jung, H.; Carrano, C. J.; Haygood, M. G.; Butler, A. Self-assembling amphiphilic siderophores from marine bacteria. *Science* **2000**, *287*, 1245–1247.

(17) Trick, C.; Wilhelm, S. Iron-limited growth of cyanobacteria: Multiple siderophore production is a common response. *Limnol. Oceanogr.* **1994**, *39*, 1979–1984.

(18) Turner, A. A binary aqueous component model for the sediment-water partitioning of trace metals in natural waters. *Environ. Sci. Technol.* **2007**, *41*, 3977–3983.

(19) Hudson, R. J. M.; Morel, F. M. M. Trace metal transport by marine organisms: Implication of metal coordination kinetics. *Deep Sea Res.* **1993**, *40*, 129–150.

(20) Van Leeuwen, H. P.; Town, R. M.; Buffle, J.; Cleven, R. F. M.; Davison, W.; Puy, J.; van Riemsdijk, W. H.; Sigg, L. Dynamic speciation analysis and bioavailability of metals in aquatic systems. *Environ. Sci. Technol.* **2005**, *22*, 8545–8556.

(21) Green, S. A.; Morel, F. M. M.; Blough, N. V. Investigation of the electrostatic properties of humic substances by fluorescence quenching. *Environ. Sci. Technol.* **1992**, *26*, 294–302.

(22) Ou, X.; Chen, S.; Quan, X.; Zhao, H. Photoinductive activity of humic acid fractions with the presence of Fe(III): The role of aromaticity and oxygen groups involved in fractions. *Chemosphere* **2008**, *72*, 925–931.

(23) Ohno, T.; Amirbahman, A.; Bro, R. Parallel factor analysis of excitation-emission matrix fluorescence spectra of water soluble soil organic matter as basis for the determination of conditional metal binding parameters. *Environ. Sci. Technol.* **2008**, *42*, 186–192.

(24) Yamashita, Y.; Jaffé, R. Characterizing the interactions between trace metals and dissolved organic matter using excitation-emission matrix and parallel factor analysis. *Environ. Sci. Technol.* **2008**, *42*, 7374–7379.

(25) Benner, R. Chemical composition and reactivity. In *Biogeochemistry of Marine Dissolved Organic Matter*; Hansell, D. A., Carlson, C. A., Eds. Academic Press: Amsterdam, 2002; pp 59−90.

(26) Tiller, C. L.; O'Melia, C. R. Natural organic matter and colloidal stability: Models and measurements. *Colloids Surf., A* **1993**, *73*, 89–102.

(27) Muller, F. L. L. Colloid/solution partitioning of metal-selective organic ligands and its relevance to Cu, Pb and Cd cycling in the Firth of Clyde. *Estuarine, Coast. Shelf Sci.* **1998**, *46*, 419–437.

(28) Krachler, R.; Krachler, R. F.; von der Kammer, F.; Süphandag, A.; Jirsa, F.; Ayromlou, S.; Hofmann, T.; Keppler, B. K. Relevance of peat-draining rivers for the riverine input of dissolved iron into the ocean. *Sci. Total Environ.* **2010**, 2402–2408.

(29) Pokrovsky, O. S.; Schott, J. Iron colloids/organic matter associated transport of major and trace elements in small boreal rivers and their estuaries (NW Russia). *Chem. Geol.* **2002**, 141–179.

ES101081C